PHYSICAL REVIEW A VOLUME 28, NUMBER 4 OCTOBER 1983

Exact second Born calculations for electron capture for systems with various projectile and target charges

J. H. McGuire* and J. Eichler
Fachbereich Physik, Hahn-Meitner Institut, D-1000 Berlin 39, West Germany

P. R. Simony
Department of Physics, Kansas State University, Manhattan, Kansas 66506
(Received 1 April 1983; revised manuscript received 13 June 1983)

Results of exact numerical calculations of differential and total $1s$-$1s$ electron-capture cross sections evaluated in the second Born approximation are presented for targets and projectiles of various charges Z_T and Z_P at velocities between 10 and 200 MeV/amu. For symmetric systems with $Z_P=Z_T=Z$ the Thomas peak in the differential cross section, characteristic of a free-wave second Born-approximation process, appears at velocities above $Z^2\times$(5 MeV/amu), where Z is the nuclear charge of the target (or projectile). The shape of this Thomas peak contains information about real and virtual intermediate states of the system. For total cross sections at velocities below $Z^2\times$(2 MeV) the second Born-approximation cross section is larger than the first Born-approximation cross section indicating a breakdown of the second Born approximation using the free-wave Green's function. Results using the peaking approximation of Drisko converge to our exact second Born-approximation results only at velocities well above $Z^2\times$(10 MeV/amu). For systems asymmetric in Z_P and Z_T no exact scaling is found, although the systematics are qualitatively similar to the symmetric case using $Z=\frac{1}{2}(Z_P+Z_T)$. For p + Ne at 100 MeV, the exact Born-approximation results lie somewhat above exact impulse-approximation calculations. It is found that the peaking approximation of Briggs and Simony converges to exact second Born-approximation results as the asymmetry of the projectile and target charges increases. At very high velocities the peaking approximation of Drisko also converges slowly to the exact second Born-approximation result.

I. INTRODUCTION

Electron capture has the unusual feature that the second term in the Born-approximation series dominates over all other orders at high velocities. The total cross section decreases[1,2] asymptotically as v^{-11} in second order, as compared to v^{-12} in first order. The v^{-11} dependence at high velocities arises due to a simple two-step mechanism[3] suggested long ago by Thomas. This Thomas mechanism, where the electron is first scattered into 60° by the projectile and then rescattered by the target nucleus, is associated with a peak in the differential scattering cross section at a center of mass angle of $\sin(60°)/M_P$ where M_P is the mass of the projectile (in atomic units). It is this Thomas peak that gives rise[1,4] to the v^{11} second Born-approximation behavior at high velocity. Recently this Thomas peak was observed[5] to emerge in H^+ + He above about 5 MeV/amu as predicted.[6,7]

Interest in the nature of electron capture at high velocities has led to a number of articles[8-21] using various approximations related to the exact second Born-approximation calculations. In a recent paper, the real and imaginary parts of the second Born-approximation amplitudes have been interpreted[22] in terms of contributions from off-energy-shell and on-energy-shell intermediate states, respectively. Furthermore, useful peaking approximations[2,11,18,20] have been introduced to simplify evaluation of the cross sections. In general, the differences in various calculations tend to be most evident in predictions of the shape of the Thomas peak, particularly at those velocities where the Thomas peak first emerges. However, most calculations have done for H^+ + H, so that very little is known about how the nature of high-velocity electron-capture cross sections, including differential cross sections, varies for different targets and projectiles.

In the past few years, significant progress has been achieved in understanding electron capture at high velocities, particularly for systems asymmetric in the projectile and target nuclear charges, Z_P and Z_T, where the strong potential approximation[11,20] applies.

In an exact formulation[20] the transition matrix for electron capture may be written as $T=V_P+V_PGV_T$ where V_P (V_T) is the interaction of the electron with the projectile (target) and G is the full Green's function. It is evident that if the exact intermediate states of the system, which are propagated by G, are known then the cross section can be computed exactly. In the strong potential approximation,[20] the T matrix is expanded in powers of Z_P/Z_T (or its inverse) and truncated after the first term. It has been shown that this corresponds to approximating G by G_C, the Coulomb Green's function. Thus the intermediate states of the systems correspond to Coulomb waves propagating in the field of the strong potential, V_T (or V_P in the inverse expansion). In the second Born approximation,[18] G is approximated by G_0, the plane-wave Green's function and the intermediate states of the system are represented

by plane waves, so that the influence of V_T on intermediate states is ignored.

At present no exact calculation within the strong potential approximation has been reported, although an exact calculation[7] in the closely related impulse approximation has been reported for $p+H$ at 10 MeV and $p+Ne$ at 100 MeV. On the other hand, a number of strong potential calculations[11,20,23] has been reported using a peak approximation devised by Briggs[11] (in the impulse approximation) and by Simony[18] (in the second Born approximation). This useful Briggs-Simony (BS) peaking approximation is valid for asymmetric systems.

In this paper exact second Born-approximation cross sections are presented and compared to results in the BS peaking approximation. Furthermore, convergence of the somewhat different Drisko peaking approximation[7,16] to an exact second Born approximation is considered. The exact second Born-approximation results are compared to recent exact impulse approximation calculations. Emphasis is given to differential cross sections, especially to the emergence of the Thomas peak, which arises due to intermediate states near the intermediate 60° state described[3] classically by Thomas.

Since detailed balance holds,[18] the results for $1s$-$1s$ capture presented here for $H^+ + A \rightarrow H + A^+$ where A is an atom, may be applied to the time reversed case, namely $A^+ + H \rightarrow A + H^+$.

II. FORMULATION

An exact expression[20] for the differential cross section may be expressed as

$$\frac{d\sigma}{d\Omega} = \frac{\mu_i \mu_f}{4\pi^3} \frac{k_f}{k_i} \left| T_{if}^{I} + T_{if}^{II} \right|^2 , \tag{1}$$

where

$$T_{if}^{I} = \langle \phi_f \mid V_f \mid \phi_i \rangle \tag{2a}$$

and

$$T_{if}^{II} = \langle \phi_f \mid V_f G^+ V_i \mid \phi_i \rangle . \tag{2b}$$

Here ϕ_i and ϕ_f are the initial and final asymptotic states, V_i and V_f the initial end final potentials, μ_i and μ_f the initial and final reduced masses, k_i and k_f the initial and final momenta, and G the exact Green's function.

Here the potential V_i (or V_f) is taken to be the Coulomb interaction, V_{BK} (sometimes referred to as the Brinkman-Kramers potential), between the active electron and the projectile (or target) nucleus. The second Born approximation is defined by taking $G \simeq G_0$, the free-wave Green's function. While other choices for V and G are possible, the leading order second Born-approximation terms at very high velocities are given by V_{BK} and G_0.

Various methods[16,18,24] are now available to reduce the expression for the second Born-approximation amplitude to a two- or a three-dimensional integral. We use the technique described in detail by Simony[18] which requires numerical integration over three dimensions. We emphasize that at high velocity, i.e., the velocities considered here, the integrand is sharply peaked and it is important to fit the numerical integration to the integrand in the region of the peaks. Despite the existence of alternate, possibly more efficient, techniques[16,24] now, no other exact second Born-approximation calculation at these high velocities has been reported to confirm or to challenge our exact second Born-approximation results, although our exact results do converge slowly to Drisko's high-velocity limit.[2]

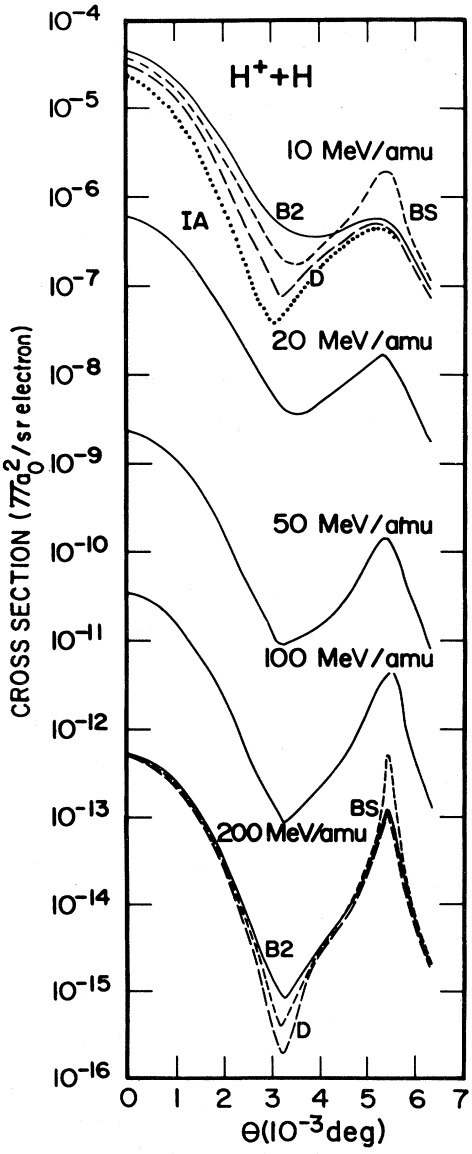

FIG. 1. Differential $1s$-$1s$ electron-capture cross section vs angle in degrees in the center of mass for $H^+ + H$ at various laboratory energies in units of πa_0^2 per electron per sr. Solid curve corresponds to exact second Born-approximation calculations, long dash to the Drisko peaking approximation, and short dash to the Briggs-Simony peaking approximation. Dotted curve represents the exact impulse approximation calculation of Ref. 7.

III. RESULTS

A. Symmetric systems

Here we present calculations for $1s$-$1s$ electron capture for symmetric Z systems for $Z=1-10$ and velocities between 10 and 200 MeV/amu, where $1s$-$1s$ capture is expected to be the dominant contribution to the total capture cross sections. Above 200 MeV/amu we estimate that relativistic effects are greater than 20% based on relativistic first Born-approximation calculations for $H^+ + H$ by Moiseiwitsch and Stockman.[25] In our calculations the wave function of the active $1s$ target electron is approximated by a hydrogenic wave function with an effective charge of $Z_T^* = Z - \frac{5}{16}$. The binding energy of the active electron is taken as $\frac{1}{2}Z_T^{*2}$. The projectile is assumed to be bare.

Differential cross sections at 10, 20, 50, 100, and 200 MeV/amu are shown for $Z=1$, 2, 4, 6, 8, and 10 in Figs. 1–6. As the velocity increases, the cross sections decrease

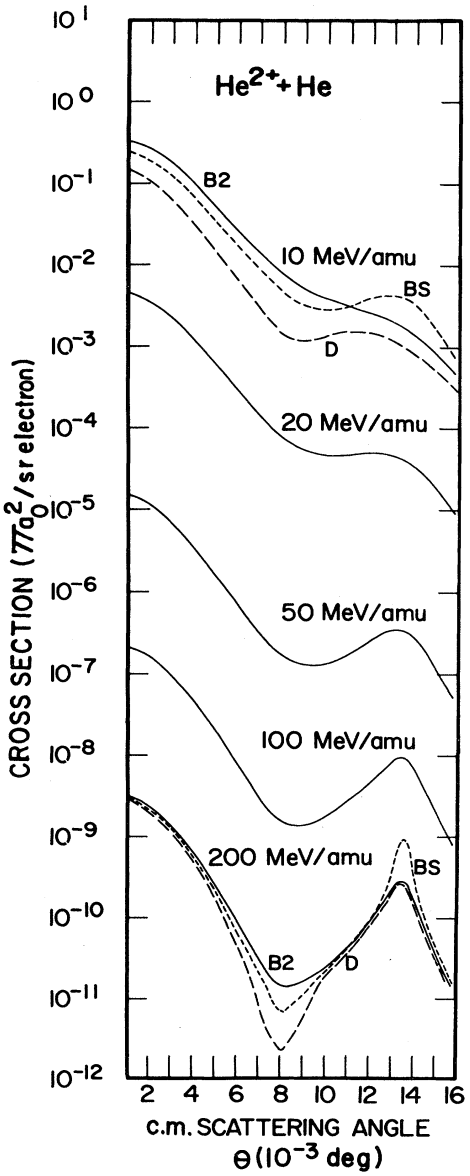

FIG. 2. Differential $1s$-$1s$ electron-capture cross section vs angle in degrees in the center of mass for $He^{2+}+He$ at various laboratory energies in units of πa_0^2 per electron per sr. Solid curve corresponds to exact second Born-approximation calculations, long dash to the Drisko peaking approximation, and short dash to the Briggs-Simony peaking approximation.

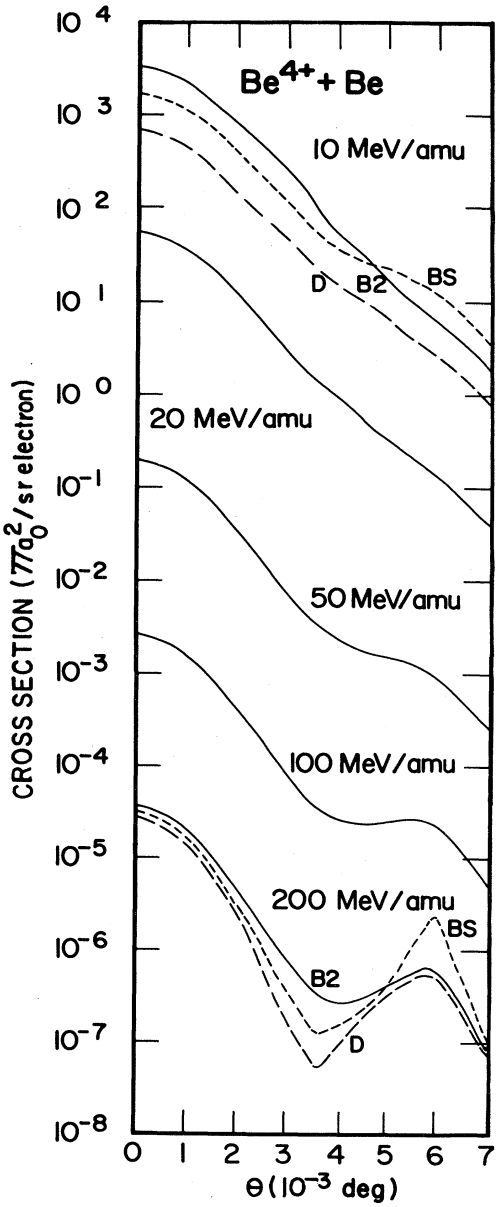

FIG. 3. Differential $1s$-$1s$ electron-capture cross section vs angle in degrees in the center of mass for $Be^{4+}+Be$ at various laboratory energies in units of πa_0^2 per electron per sr. Solid curve corresponds to exact second Born-approximation calculations, long dash to the Drisko peaking approximation, and short dash to the Briggs-Simony peaking approximation.

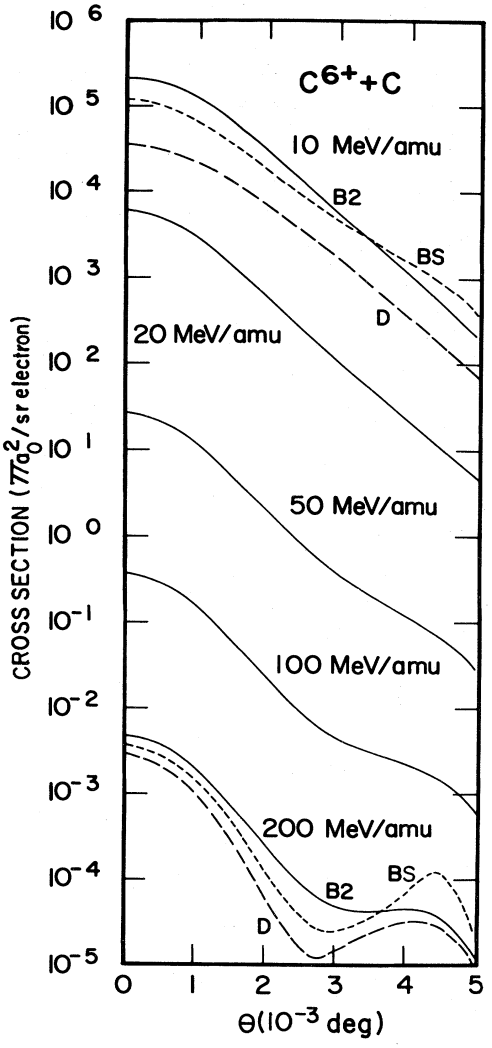

FIG. 4. Differential 1s-1s electron-capture cross section vs angle in degrees in the center of mass for $C^{6+}+C$ at various laboratory energies in units of πa_0^2 per electron per sr. Solid curve corresponds to exact second Born-approximation calculations, long dash to the Drisko peaking approximation, and short dash to the Briggs-Simony peaking approximation.

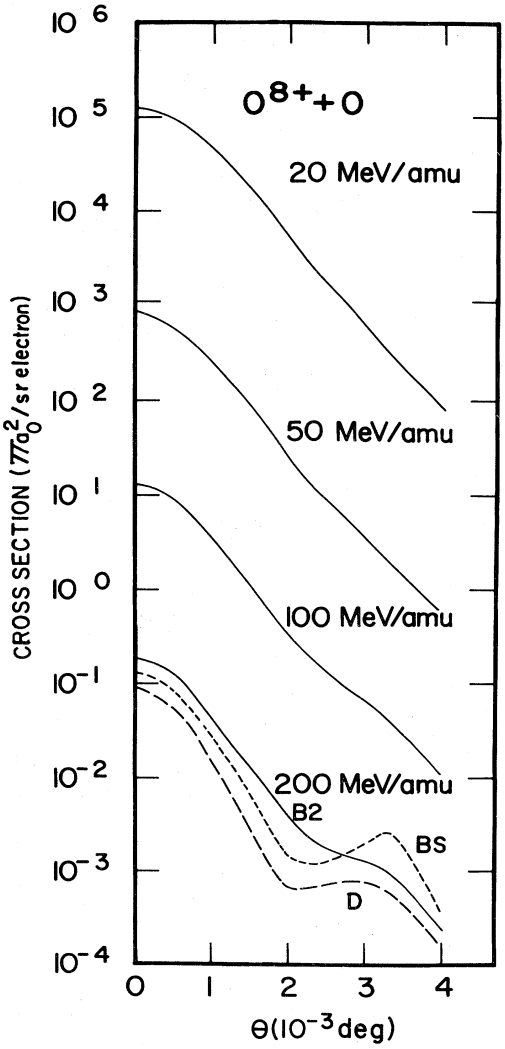

FIG. 5. Differential 1s-1s electron-capture cross section vs angle in degrees in the center of mass for $O^{8+}+O$ at various laboratory energies in units of πa_0^2 per electron per sr. Solid curve corresponds to exact second Born-approximation calculations, long dash to the Drisko peaking approximation, and short dash to the Briggs-Simony peaking approximation. Results at 10 MeV/amu are not available.

rapidly. However, the Thomas peak at $\theta_T=\sin(60°)/M_P$ decreases less rapidly than the forward peak. The area under this Thomas peak varies as v^{-11}, as compared to v^{-12} for the forward peak at asymptotic velocities so that eventually the Thomas peak dominates the entire cross section. As Z increases, the Thomas peak emerges at higher velocities. This occurs because Z, which is equal to the velocity of the K-shell electron, sets the velocity scale for this process. Hence the peak tends to emerge at a constant value of v/Z, as discussed later.

The shape of the Thomas peak depends on several factors. At the higher velocities where the Thomas peak is well separated from the forward peak, the Thomas peak is determined entirely by the second term, T_{if}^{II}, in Eq. (1), i.e., the first Born-approximation amplitude is negligible. The amplitude T_{if}^{II} has both a real and an imaginary part. The term $\mathrm{Im}T_{if}^{II}$ corresponds[22] to intermediate states that conserve energy. It has been shown[1,4] that at high velocities one state dominates—namely that state where the electron has been scattered into a 60° angle as described by the classical Thomas model. It is this term which is dominant at the Thomas angle, θ_T. The term $\mathrm{Re}T_{if}^{II}$ corresponds to intermediate states that do not conserve energy, consistent with the uncertainty principle, i.e., virtual intermediate states. At θ_T the term $\mathrm{Re}T_{if}^{II}$ changes sign and is therefore zero. However, even in the asymptotic veloci-

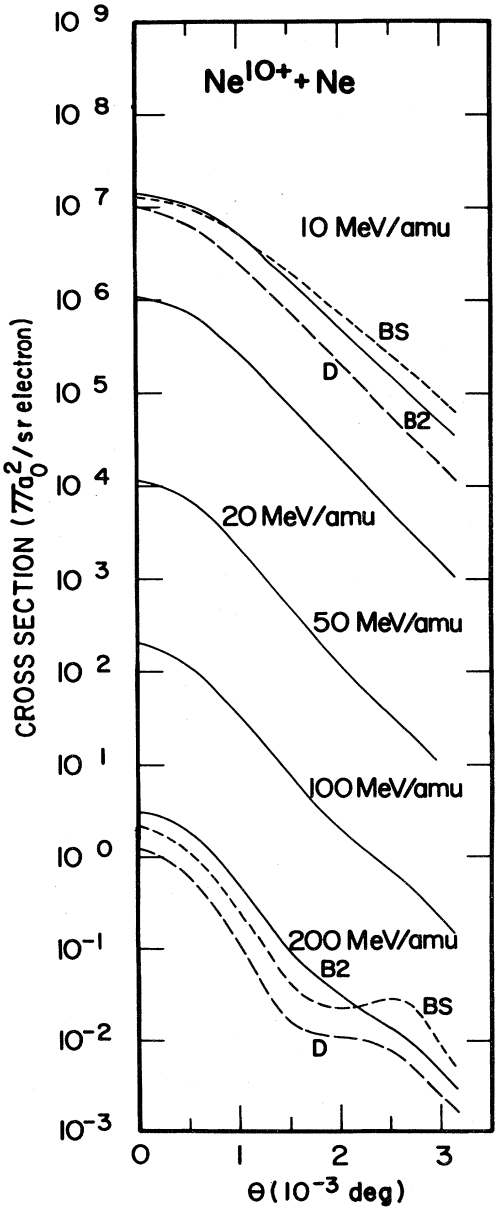

FIG. 6. Differential 1s-1s electron-capture cross section vs angle in degrees in the center of mass for $Ne^{10+}+Ne$ at various laboratory energies in units of πa_0^2 per electron per sr. Solid curve corresponds to exact second Born-approximation calculations, long dash to the Drisko peaking approximation, and short dash to the Briggs-Simony peaking approximation.

ty limit, $\mathrm{Re}T_{if}^{II}$ amplitudes from angles near (but not at) θ_T contribute[22] as much to the total cross section as does $\mathrm{Im}T_{if}^{II}$. Hence the virtual intermediate states which cannot be described classically contribute significantly to the cross section by affecting the shape of the Thomas peak.

At the lower velocities the Thomas peak broadens. This corresponds to a broader distribution of intermediate states, both on shell and off shell, as is evident[22] from an examination of the amplitudes $\mathrm{Re}T_{if}^{II}$ and $\mathrm{Im}T_{if}^{II}$. Furthermore, at a velocity of about $Z^2\times(1$ MeV/amu) the sign of $\mathrm{Re}T_{if}^{II}$ changes. Above this velocity, $\mathrm{Re}T_{if}^{II}$ and T_{if}^{I} (which is real) have opposite signs and interfere destructively. The dip in the differential cross section tends to occur where $\mathrm{Re}T_{if}^{II}+T_{if}^{I}=0$ (with $\mathrm{Im}T_{if}^{II}\neq 0$). However, below $Z^2\times(1$ MeV/amu), $\mathrm{Re}T^{II}$ and T_{if}^{I} interfere constructively. As a result the second Born-approximation cross section is larger than the first Born-approximation (BK) cross section, which typically lies above the data. It has been

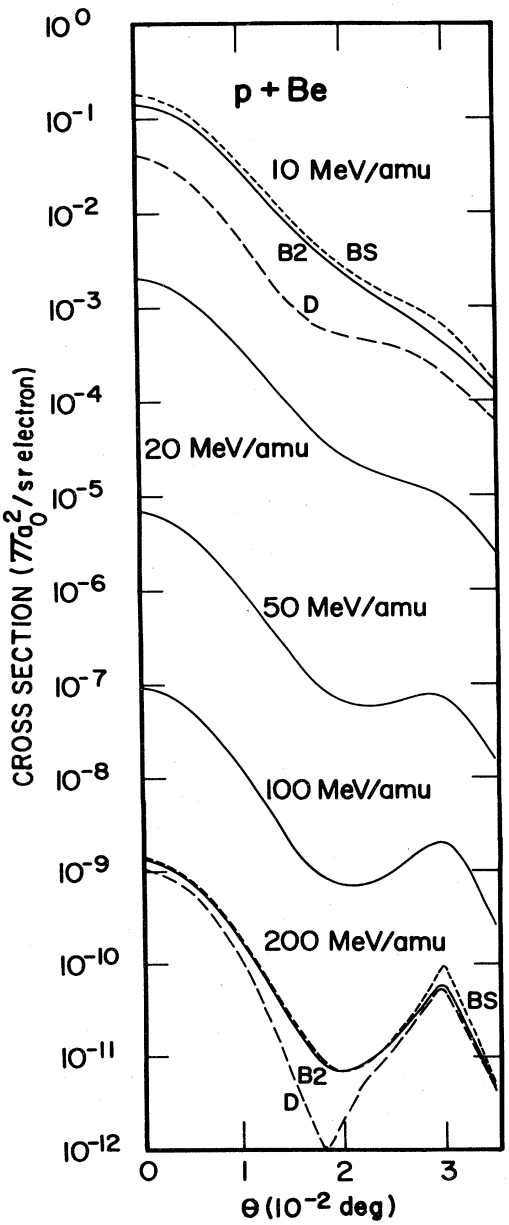

FIG. 7. Differential 1s-1s electron-capture cross section vs angle in degrees in the center of mass for $H^+ + Be$ at various laboratory energies in units of πa_0^2 per electron per sr. Solid curve corresponds to exact second Born-approximation calculations, long dash to the Drisko peaking approximation, and short dash to the Briggs-Simony peaking approximation.

TABLE I. Total $1s$-$1s$ electron-capture cross sections in the first Born (B1) and second Born (B2) approximations in units of πa_0^2 per electron at various laboratory energies for systems symmetric in projectile and target charges.

Energy	$H^+ + H$		$He^{2+} + He$		$Be^{4+} + Be$	
(MeV/amu)	B1	B2	B1	B2	B1	B2
10	1.21(−11)	8.04(−12)	4.71(−09)	4.84(−09)	4.46(−06)	9.36(−06)
20	1.94(−13)	1.13(−13)	8.00(−11)	6.25(−11)	9.72(−08)	1.44(−07)
50	8.07(−16)	4.51(−16)	3.45(−13)	2.11(−13)	4.92(−10)	4.74(−10)
100	1.27(−17)	7.52(−18)	5.48(−16)	3.09(−15)	8.26(−12)	6.14(−12)
200	1.98(−19)	1.33(−19)	8.64(−17)	4.87(−17)	1.34(−13)	8.31(−14)
Energy	$C^{6+} + C$		$O^{8+} + O$		$Ne^{10+} + Ne$	
10	1.36(−04)	4.15(−04)	1.08(−03)	3.5 (−03)	3.66(−03)	1.42(−02)
20	4.19(−06)	9.43(−06)	4.58(−05)	1.34(−04)	2.35(−04)	8.12(−04)
50	2.71(−08)	3.86(−08)	4.01(−07)	7.69(−07)	2.87(−06)	6.86(−06)
100	4.98(−10)	5.11(−10)	8.31(−09)	1.12(−08)	6.84(−08)	1.16(−07)
200	8.46(−12)	6.60(−12)	1.50(−10)	1.47(−10)	1.34(−09)	1.61(−09)

pointed out[22] that this could be due to an absence of low-lying off-energy-shell intermediate states, such as bound states which are not present in our second Born-approximation calculations, but which are included in the strong potential approximation.

Two peaking approximations, described in detail elsewhere,[18] are also plotted in these figures at 10 and 200 MeV/amu. The Drisko peaking approximation is the standard peaking approximation applied to second Born-approximation calculations for electron capture. This Drisko peaking approximation is designed to calculate the cross section accurately in the vicinity of the Thomas peak. In this approximation the Green's function is linearized in an expansion in the momentum of intermediate states about the Thomas state. Hence contributions far away from the Thomas peak (e.g., the forward peak) are not accurately included. It is evident from the figures that in the vicinity of the Thomas peak our calculations converge slowly to the Drisko peaking approximation as the velocity increases.

The second peaking approximation is due to Briggs[11] and to Simony,[18] and is applicable to systems asymmetric in the projectile and target charges. In this approximation one expands the intermediate momentum about the momentum of the initial (or final state) wave function (whichever is more sharply peaked). This approximation is accurate at forward angles or small momentum transfer, especially for asymmetric systems. It is evident from the figures that this peaking approximation is reasonable for the forward peak. However, the Thomas peak is overemphasized in the symmetric systems shown here, and at high velocities there are large, i.e., factor of 2, differences between this Briggs-Simony peaking approximation and the exact result.

In Fig. 1 for $H^+ + H$ at 10 MeV are shown results of exact calculations[7] in the impulse approximation (i.e., without peaking approximation) which are now available. It is expected that these results will be close to exact calculations in the strong potential approximation[20] (which are not now available). It is noted that the exact impulse calculations lie below our second Born-approximation calculations and give a more pronounced Thomas peak. We also note that, especially near the Thomas peak, the Drisko peaking approximation lies reasonably close to the exact impulse approximation. This Drisko peaking approximation also lies close to the differential cross sections evaluated in the continuum distorted-wave (CDW) approximation for $H^+ + H$, except that the CDW calculations[12] have a sharp dip in the middle of the Thomas peak. This dip is associated with interference between Coulomb distorted initial and final stages at large impact parameters.

In Table I total cross sections are listed for the systems shown in Figs. 1—6. Here first Born-approximation (BK)

TABLE II. Total $1s$-$1s$ electron-capture cross sections in the first Born (B1) and second Born (B2) approximations in units of πa_0^2 per electron at various laboratory energies for systems asymmetric in projectile and target charges.

Energy	$H^+ + Be$		$H^+ + C$		$H^+ + O$		$H^+ + Ne$	
(MeV/amu)	B1	B2	B1	B2	B1	B2	B1	B2
10	6.07(−09)	9.81(−09)	3.41(−08)	9.74(−08)	8.48(−08)	3.0 (−07)	1.30(−07)	8.60(−07)
20	1.31(−10)	1.29(−10)	7.87(−10)	1.51(−09)	2.59(−09)	7.71(−09)	5.55(−09)	2.39(−08)
50	5.16(−13)	4.06(−13)	4.11(−12)	4.88(−12)	1.63(−11)	2.48(−11)	4.37(−11)	1.07(−11)
100	8.36(−15)	5.46(−15)	6.97(−14)	6.13(−14)	2.94(−13)	3.56(−13)	8.59(−13)	1.41(−12)
200	1.33(−16)	7.91(−17)	1.13(−15)	8.01(−16)	4.95(−15)	4.41(−15)	1.51(−14)	1.72(−14)

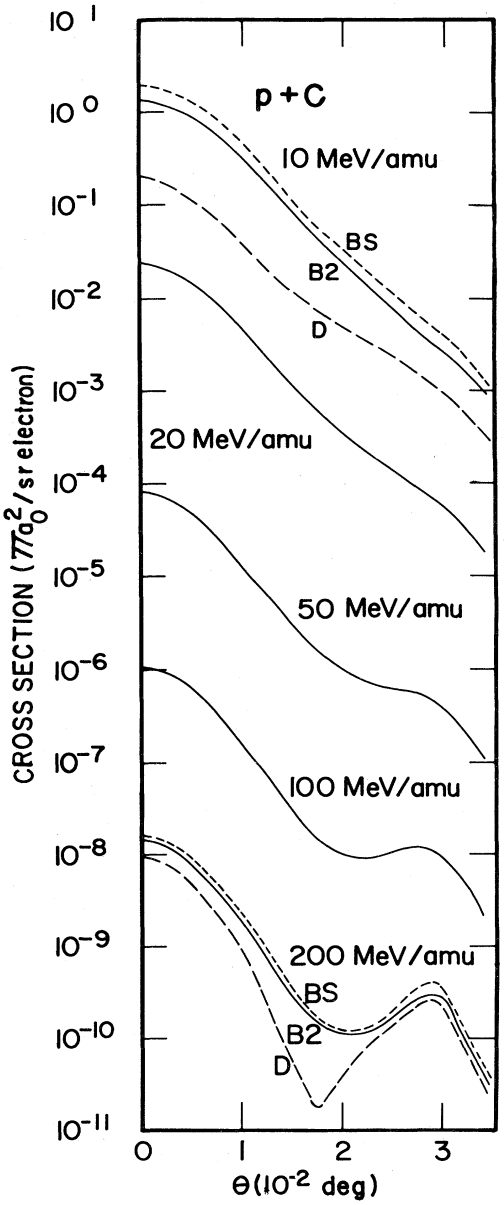

FIG. 8. Differential $1s$-$1s$ electron-capture cross section vs angle in degrees in the center of mass for $H^+ + C$ at various laboratory energies in units of πa_0^2 per electron per sr. Solid curve corresponds to exact second Born-approximation calculations, long dash to the Drisko peaking approximation, and short dash to the Briggs-Simony peaking approximation.

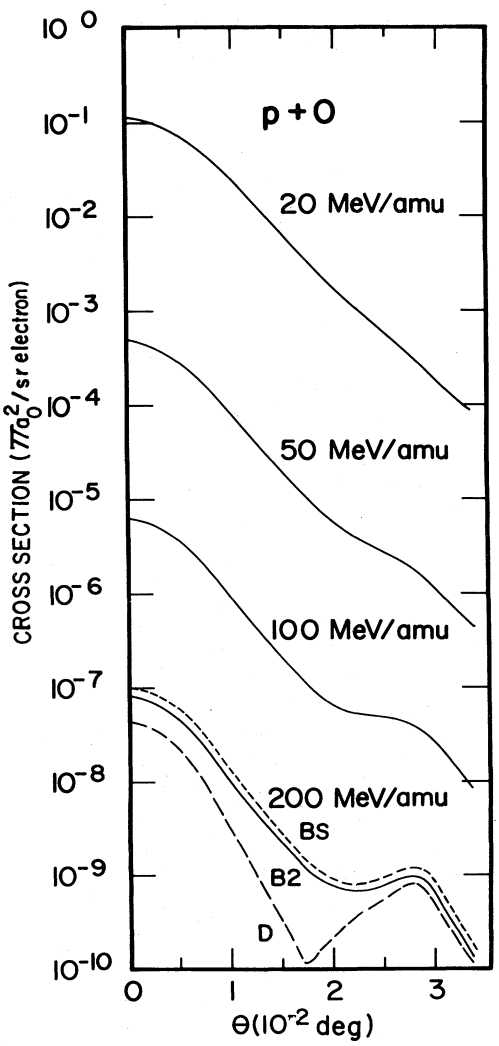

FIG. 9. Differential $1s$-$1s$ electron-capture cross section vs angle in degrees in the center of mass for $H^+ + O$ at various laboratory energies in units of πa_0^2 per electron per sr. Solid curve corresponds to exact second Born-approximation calculations, long dash to the Drisko peaking approximation, and short dash to the Briggs-Simony peaking approximation. Results at 10 MeV/amu are not available.

and exact second Born-approximation cross sections are tabulated. At velocities below $Z^2\times(2$ MeV/amu) the second Born-approximation cross section is larger than the first Born-approximation (BK) cross section. Since the first Born-approximation (BK) cross section lies above observation, this indicates a breakdown of the second Born approximation.

B. Asymmetric systems

Here we present calculations for $1s$-$1s$ electron capture for $p + Be$, $p + C$, $p + O$, and $p + Ne$ at velocities between 10 and 200 MeV where $1s$-$1s$ capture is expected to be the dominant-contribution to the total capture cross sections. Differential cross sections at 10, 20, 50, 100, and 200 MeV are shown for $Z_T = 4$, 6, 8, and 10 in Figs. 7–11. As Z_T increases, the Thomas peak again emerges at higher velocities. This occurs because Z_T, which is equal to the velocity of the K-shell electron, sets the velocity scale for this process. The peak does not emerge at a constant value of v/Z_T, however.

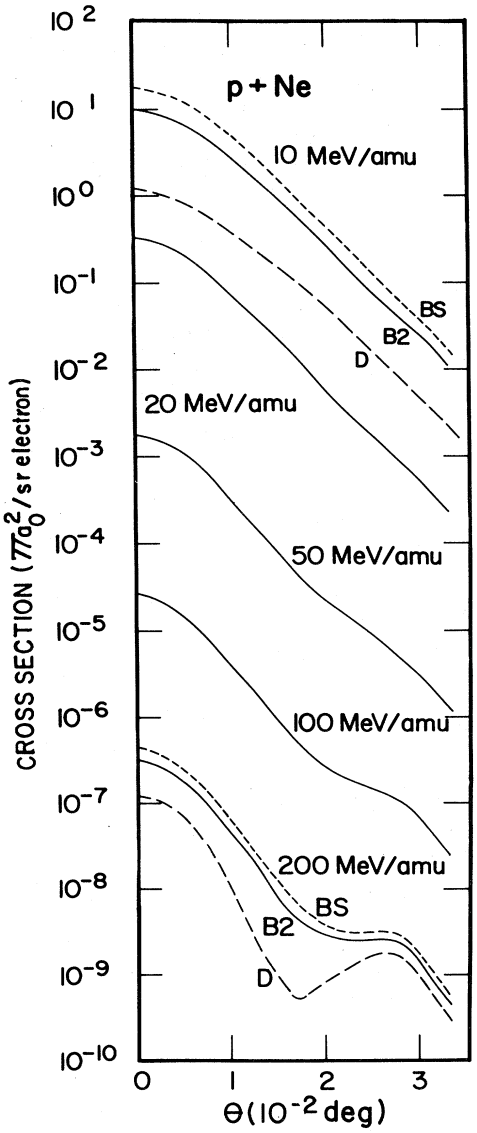

FIG. 10. Differential 1s-1s electron-capture cross section vs angle in degrees in the center of mass for $H^+ + Ne$ at various laboratory energies in units of πa_0^2 per electron per sr. Solid curve corresponds to exact second Born-approximation calculations, long dash to the Drisko peaking approximation, and short dash to the Briggs-Simony peaking approximation.

The two peaking approximations, described above, are also plotted in these figures at 10 and 200 MeV/amu. It is evident from the figures that in the vicinity of the Thomas peak our calculations again converge slowly to the Drisko peaking approximation as the velocity increases. However, it is now evident that Briggs-Simony peaking approximation does converge to the exact second Born-approximation results in the limit as Z_P/Z_T goes to zero even at the lower velocities shown. It is noted that this BS peaking approximation does not satisfy detailed balancing, and that the BS peaking approximation is much more accurate for $Ne^+ + H \rightarrow Ne + H^+$ than for $H^+ + Ne \rightarrow H + Ne^+$. The calculation shown was done for $Ne^+ + H \rightarrow Ne + H^+$.

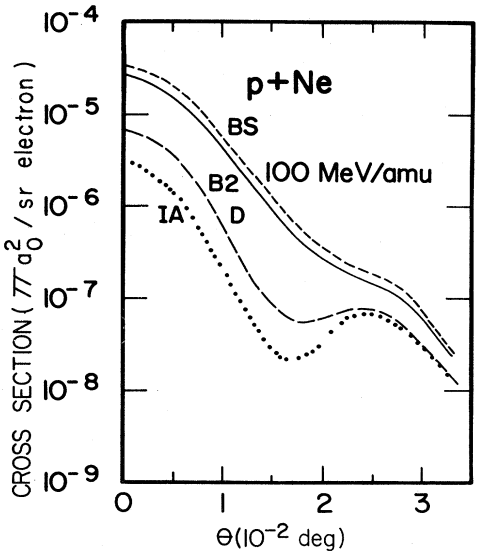

FIG. 11. Differential cross sections at 100 MeV for $p + Ne$. The solid, long dash, and short dash curves represent exact second Born, Drisko peaked second Born, and Briggs-Simony peaked second Born approximations, respectively, as in Fig. 4. Dotted curve represents exact impulse results.

In Table II total cross section are listed for the systems shown in Figs. 1—5. Here first Born-approximation (BK) and exact second Born-approximation cross sections are tabulated. It is more difficult to isolate features in these total cross sections that illustrate the influence of the second Born-approximation terms than in the more detailed differential cross section where the Thomas peak is evident.

Various effects are omitted in our results for both symmetric and asymmetric systems. Radiative electron capture,[26] which as discussed in an earlier paper[6] is expected to be dominant at the higher velocities, has not been included. Coulomb deflection by the nucleus has also been ignored. However, it is not expected[6] that this effect is important except at angles larger than the Thomas angle. And rescattering of the active electron from its intermediate state by other electrons in the target has been ignored. It has been pointed out[27,28] that this could give rise to a second peak at angles somewhat larger than the Thomas angle. However, as previously discussed,[6] we expect this effect to be small based on a calculation by Briggs and Taulbjerg.[28]

IV. SUMMARY

Calculations of 1s-1s electron capture cross sections in the second Born approximation have been presented for systems both symmetric and asymmetric in the projectile and target charge Z. At high velocities a peak appears in the differential cross section at the Thomas angle

$\theta_T = \sin(60°)/M_P$. The shape of this Thomas peak contains information about the distribution of real and virtual intermediate states through which the system passes in a two-step process. The peaking approximation of Drisko converges slowly to the exact second Born-approximation results as the velocity increases. For symmetric systems the peaking approximation of Briggs and Simony does not converge to the exact second Born-approximation results. However, for the asymmetric systems, the peaking approximation of Briggs and Simony does converge to the exact second Born-approximation results in the limit as Z_P/Z_T goes to zero. For the p +Ne at 100 MeV, there is reasonable agreement between our exact second Born-approximation results and differential cross sections evaluated in the exact impulse approximation, and the second Born approximation lies slightly above the impulse approximation as expected. Finally, it is estimated that the nonrelativistic second Born approximation is valid only for systems with Z_T less than 10 in a velocity region above at least several MeV/amu where the second Born-approximation total cross sections are smaller than first order Brinkman-Kramer cross sections, and below 200 MeV/amu where relativistic effects become significant.

ACKNOWLEDGMENTS

Assistance of R. Kletke is gratefully acknowledged. This work was supported in part by the U. S. Department of Energy, Division of Chemical Sciences.

*Permanent address: Department of Physics, Kansas State University, Manhattan, KS 66506.

[1]R. Shakeshaft and L. Spruch, Rev. Mod. Phys. 51, 369 (1979).
[2]R. M. Drisko, Ph.D. thesis, Carnegie Institute of Technology (unpublished).
[3]L. H. Thomas, Proc. R. Soc. London Ser. A 114, 561 (1927).
[4]J. Eichler and H. Narumi, Z. Phys. A 295, 209 (1980).
[5]C. L. Cocke, E. Horsdal-Pedersen, and M. Stoeckli, Phys. Rev. Lett. 50, 1910 (1983).
[6]P. R. Simony, J. H. McGuire, and J. Eichler, Phys. Rev. A 26, 1337 (1982).
[7]J. S. Briggs, P. T. Greenland, and L. Kocbach, J. Phys. B 15, 3805 (1982).
[8]J. S. Briggs and L. Dube, J. Phys. B 13, 771 (1980).
[9]R. Shakeshaft, Phys. Rev. Lett. 44, 442 (1980).
[10]J. Macek and K. Taulbjerg, Phys. Rev. Lett. 46, 170 (1981).
[11]J. S. Briggs, J. Phys. B 10, 3075 (1977); private communication.
[12]J. E. Maraglia, R. D. Piacentini, R. D. Riverola, and A. Salin, J. Phys. B 14, 1191 (1981).
[13]L. Kocbach, J. Phys. B 13, 1665 (1980).
[14]P. A. Amundsen and D. Jakubassa, J. Phys. B 13, 1467 (1980).
[15]P. J. Kramer, Phys. Rev. A 6, 2125 (1972).
[16]J. M. Wadehra, R. Shakeshaft, and J. H. Macek, J. Phys. B 14, L767 (1981).
[17]P. R. Simony and J. H. McGuire, J. Phys. B 14, L737 (1981).
[18]P. R. Simony, Ph.D. thesis, Kansas State University, 1981 (unpublished).
[19]P. R. Simony and J. H. McGuire, *Proceedings of the 7th International Conference of Atomic and Molecular Physics, Cambridge, August, 1980,* edited by D. Kleppner and F. M. Pipkin (Plenum, New York, 1981).
[20]J. Macek and S. Alston, Phys. Rev. A 26, 250 (1982).
[21]M. R. C. McDowell and J. P. Coleman, *Introduction to the Theory of Ion-Atom Collisions* (North-Holland, Amsterdam, 1970), Chap. 8.
[22]J. H. McGuire, P. R. Simony, O. L. Weaver, and J. Macek, Phys. Rev. A 26, 1109 (1982).
[23]J. H. McGuire, IEEE NS-30, 1100 (1983).
[24]N. C. Sil, private communication.
[25]B. L. Moiseiwitsch and S. G. Stockman, J. Phys. B 13, 2975 (1980).
[26]M. Kleber and D. H. Jakubassa, Nucl. Phys. A 252, 152 (1975).
[27]R. Shakeshaft and L. Spruch, J. Phys. B 11, L457 (1978).
[28]J. S. Briggs and K. Taulbjerg, J. Phys. B 12, 2565 (1979).